Tropical cyclones and the ecohydrology of Australia's recent continental-scale drought

Gavan S. McGrath,[1] Rohan Sadler,[2] Kevin Fleming,[3,4] Paul Tregoning,[5] Christoph Hinz,[1,6] and Erik J. Veneklaas[7]

Received 8 November 2011; revised 20 December 2011; accepted 22 December 2011; published 9 February 2012.

[1] The Big Dry, a recent drought over southeast Australia, began around 1997 and continued until 2011. We show that between 2002–2010, instead of a localized drought, there was a continent-wide reduction in water storage, vegetation and rainfall, spanning the northwest to the southeast of Australia. Trends in water storage and vegetation were assessed using Gravity Recovery and Climate Experiment (GRACE) and Normalized Difference Vegetation Index (NDVI) data. Water storage and NDVI are shown to be significantly correlated across the continent and the greatest losses of water storage occurred over northwest Australia. The frequency of tropical cyclones over northwest Australia peaked just prior to the launch of the GRACE mission in 2002. Indeed, since 1981, decade-scale fluctuations in tropical cyclone numbers coincide with similar variation in rainfall and vegetation over northwest Australia. Rainfall and vegetation in southeast Australia trended oppositely to the northwest prior to 2001. Despite differences between the northwest and southeast droughts, there is reason to believe that continental droughts may occur when the respective climate drivers align. **Citation:** McGrath, G. S., R. Sadler, K. Fleming, P. Tregoning, C. Hinz, and E. J. Veneklaas (2012), Tropical cyclones and the ecohydrology of Australia's recent continental-scale drought, *Geophys. Res. Lett.*, *39*, L03404, doi:10.1029/2011GL050263.

1. Introduction

[2] There has been significant focus on the causes and consequences of the so called Big Dry, a drought afflicting southeast Australia from approximately 1997 till 2011 [*Ummenhofer et al.*, 2009; *Leblanc et al.*, 2009]. This drought is regarded as a local phenomenon, particularly affecting southeast Australia. Major droughts affecting southeast Australia have been attributed to the lack of negative phases of the Indian Ocean Dipole (IOD) [*Ummenhofer et al.*, 2009; *Smith and Timbal*, 2012]. The IOD is an irregular oscillation of sea surface temperatures and atmospheric circulation in and around the Indian Ocean, characterized by the Dipole Mode Index (DMI). In the negative phase, with warmer waters off northwest Australia, the atmospheric circulation brings moisture across the continent in a southeasterly direction [*Ashok et al.*, 2003; *Ummenhofer et al.*, 2009]. In the positive phase, southeast Australia experiences lower rainfall. In early 2011, the apparent end of the drought coincided with a strong La Niña and the occurrence of a strongly negative DMI. We hypothesized that a drought in southeast Australia may therefore be associated with a continent-wide drought, oriented northwest to southeast across the continent.

[3] A warming trend in the equatorial Indian Ocean as well as a tendency for stronger and more frequent positive IOD events have been identified [*Ashok et al.*, 2003; *Ihara et al.*, 2008]. Modeling efforts also support the hypothesis of an anthropogenic contribution to more frequent positive events [*Cai et al.*, 2009]. On the other hand, there is also a suggestion that variability is on the increase, with more intense fluctuations between wet and dry states [*Abram et al.*, 2008]. Better understanding the impacts on terrestrial ecology arising from Indian Ocean variability is crucial for properly assessing whether more persistent changes are underway.

[4] An eight percent increase in the fraction of Photosynthetically Active Radiation (fPAR) absorbed by vegetation across Australia was reported to have occurred during the period 1981–2006, particularly in the central and northwestern regions [*Donohue et al.*, 2009]. This coincided with a reported increase in the frequency of extreme rainfall events in northwest Australia [*Taschetto and England*, 2009]. *Donohue et al.* [2009] also noted a northwest to southeast gradient in mean annual rainfall trends, in particular, positive trends of summer and autumn rainfall in the northwest and negative trends in the southeast. Enhanced austral winter rainfall however, is associated with a negative DMI [*Ashok et al.*, 2003] while summer and autumn rainfall in northwest Australia is associated with tropical cyclones and the monsoon.

[5] Tropical cyclones are major sources of the water which sustains vegetation in northwest Australia, resulting from the significant recharge of water stores which they induce [*Cullen and Grierson*, 2007]. Indeed, evidence for a period of desertification of the northwest was coincident with a prolonged decrease in tropical cyclone frequency [*Nott*, 2010]. Tropical cyclone frequency and intensity reportedly increased during 1980–2005 in the northwest, with no significant trends in the northeast [*Hassim and Walsh*, 2008]. However, *Goebbert and Leslie* [2010]

[1]School of Earth and Environment, University of Western Australia, Crawley, Western Australia, Australia.
[2]School of Agricultural and Resource Economics, University of Western Australia, Crawley, Western Australia, Australia.
[3]Western Australian Centre for Geodesy, Curtin University of Technology, Bentley, Western Australia, Australia.
[4]Earthquake Risk and Early Warning, Helmholtz Centre Potsdam, GFZ German Research Centre for Geosciences, Potsdam, Germany.
[5]Research School of Earth Sciences, Australian National University, Canberra, ACT, Australia.
[6]Hydrology and Water Resources Management, Brandenburg University of Technology, Cottbus, Germany.
[7]School of Plant Biology, University of Western Australia, Crawley, Western Australia, Australia.

0094-8276/12/2011GL050263

found no trends in northwest Australian cyclones between 1970–2008. *Liu and Chan* [2010] suggested that an El Niño Southern Oscillation (ENSO) interaction with IOD influenced cyclone frequency over northwest Australia. While it remains unclear whether long term trends in tropical cyclones are taking place, short term variability may have implications for the dynamics of water storage, due to the significant recharge these events can bring and the associated vegetation response. As tropical cyclones crossing land do so primarily in the north and northwest of the continent, we expect any impact on the ecohydrology to be greatest there, however more widespread impacts may also be associated with the typical southeasterly movement of the rain bearing depressions which they become.

[6] To evaluate ecohydrological dynamics in Australia, we measure trends in and correlations between water storage as measured by the Gravity Recovery and Climate Experiment (GRACE) space mission and vegetation as measured by the Advanced Very High Resolution Radiometer (AVHRR) Land and Moderate Resolution Imaging Spectroradiometer (MODIS) Terra satellites. The GRACE mission measures spatial and temporal fluctuations of the Earth's gravity field resulting from mass changes due to the movement of oceanic waters, the atmosphere, ice and soil moisture amongst others [e.g., *Wahr et al.*, 2004; *Swenson and Wahr*, 2006]. Recent studies have demonstrated the ability of GRACE to measure Australia's response to rainfall [*Rieser et al.*, 2010] as well as the southeast Australian drought [*Leblanc et al.*, 2009]. A drought more extensive than just southeast Australia, should have produced trends in water storage losses over the period of GRACE operation, 2002 to the present [*Leblanc et al.*, 2009]. Declining vegetation, consistent with the pattern of water loss, should provide independent evidence of the ecological impact of the drought. Our definition of drought encompasses long term decline in water storage with an ecological impact.

2. Data and Methods

2.1. Water Storage

[7] GRACE is a joint USA/German effort employing two low-earth orbiting satellites that use measurements of variations in their positions to infer time-variable fluctuations in the Earth's gravitational field [*Wahr et al.*, 2004]. Several gravity-field solutions are produced by various institutions which differ in the way they account for various geophysical effects (e.g. tides) and in how they apply their inversion methods to infer the gravity field from the satellites' measurements. An issue resulting from the inversion methodology is the impact of spatial and spectral leakage between the oceans and land, as well as the removal of north-south striping errors in the global spherical harmonic solutions [*Swenson and Wahr*, 2006]. To overcome some of these difficulties, various approaches are applied, including Gaussian filters. We used a global spherical harmonic solution with a 300 km radius Gaussian filter produced by the Centre for Space Research, University of Texas at Austin. The gravitational anomalies in terms of Equivalent Water Thickness (EWT) are given at a 1° resolution [*Swenson and Wahr*, 2006].

2.2. Vegetation

[8] NDVI is based upon a ratio of the red reflectance (ρ_R) and near-infrared reflectance (ρ_N), i.e., NDVI = $(\rho_N - \rho_R)/(\rho_N + \rho_R)$. NDVI is a reasonably linear measure of vegetation chlorophyll content; however it tends to saturate at dense canopy cover [*Huete et al.*, 2002]. With sparse cover, issues with reflectance can make an inter-comparison of NDVI values between locations problematic [*Huete et al.*, 2002; *Donohue et al.*, 2008]. Because we focus on areas with predominantly sparse canopies, we evaluate relative temporal trends in vegetation at a location, rather than differences in the absolute value of NDVI between sites [*Donohue et al.*, 2008, 2009]. We used the MODIS product, MOD13C2, a 0.05° monthly grid, obtained for the period 2002–2010. In addition we used monthly fPAR derived from the AVHRR Land satellite [*King*, 2003]. The fPAR grids (0.08° resolution), spanning the period 1981–2006, were used because they have been geometrically corrected and calibrated for Australia [*Donohue et al.*, 2008].

2.3. Climate Data

[9] Gridded monthly rainfall fields (0.05° resolution) were obtained from the Australian Bureau of Meteorology (BoM). In addition, best track cyclone data for the Australian area were obtained from The Australian Tropical Cyclone Database available at http://www.bom.gov.au. This data set was updated for the period 2007–2010 using data compiled by G. Padgett (unpublished data available at http://www.australiasevereweather.com/cyclones, a database derived from BoM tropical cyclone reports). The position of recent cyclone centers as they move through the Australian region are recorded to an accuracy of 0.1°. Annual tropical cyclone frequency, was calculated for a region of northwest Australia (see Section 3 for details) for the period 1969–2010. The monthly Nino3.4 anomaly was obtained from http://www.cpc.ncep.noaa.gov/data/indices/sstoi.indices while the weekly DMI was obtained from http://ioc-goos-oopc.org/state_of_the_ocean/sur/ind/dmi.php.

2.4. Trend Analyses

[10] Time series $y(t)$ were normalized as follows: $\hat{y}(t) = (y(t) - y_{\min})/(y_{\max} - y_{\min})$, where $y_{\min}$ and $y_{\max}$ are the respective minimum values and maximum values observed at a location between April 2002–April 2010. Normalized water storage and vegetation time series are denoted by $\widehat{\text{EWT}}$ and $\widehat{\text{NDVI}}$ respectively. This way the significance of trends relative to the amplitude of variation at a site could be assessed. The magnitude and significance ($p < 0.05$) of trends were quantified by linear regression and seasonal Mann–Kendall approaches [*Xu et al.*, 2005]. Both analyses gave similar results, hence only the trends from the linear regressions are presented here. Short term rainfall trends were more difficult to identify using these methods; instead a running mean monthly rainfall record, with a window of 36 months, was used to assess linear trends in rainfall. Time series of an area of northwest Australia were also smoothed using moving averages and generalized cross validation to estimate the smoothing parameters of fitted generalized additive models which decomposed the time series into seasonal and long term trends [*Wood*, 2004].

3. Results and Discussion

[11] A selection of time series from sites across Australia illustrates the close relationship between water storage and

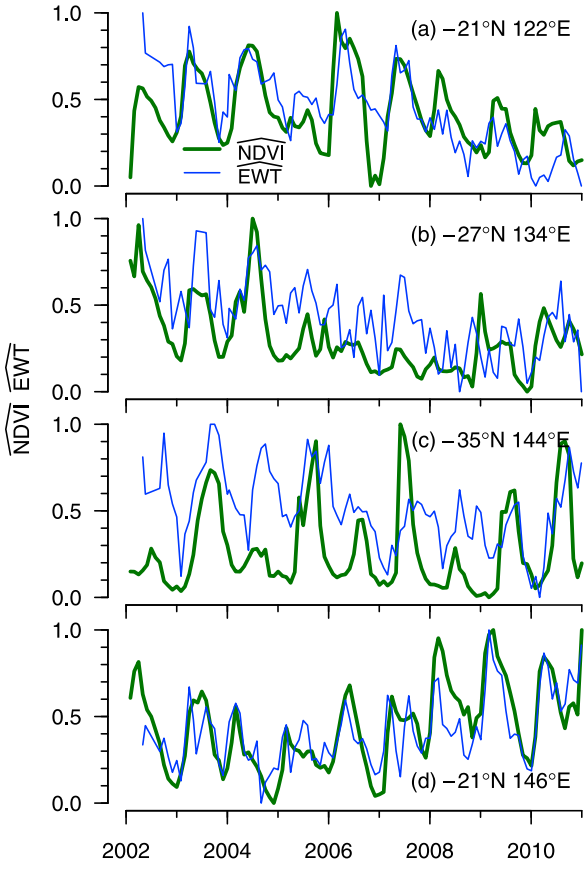

Figure 1. Time series of normalized NDVI, $\widehat{\text{NDVI}}$, and normalized EWT, $\widehat{\text{EWT}}$, at selected sites corresponding to those marked in Figure 2a.

vegetation variations (Figure 1). $\widehat{\text{EWT}}$ and $\widehat{\text{NDVI}}$ show similar levels and timing of fluctuations, particularly in the more arid regions (e.g., Figures 1a and 1b). In the more energy–limited southeast, vegetation and water storage fluctuations do not appear to be as strongly correlated (Figure 1c), however there is evidence of reasonably strong correlations there too. Figure S1 in the auxiliary material summarizes the spatial distribution of cross-correlation coefficients, ρ, for Australia.[1] This indicates $\rho > 0.8$ in the north of Australia, and often $\rho > 0.7$ in northwest and north-central Australia, as well as some parts of southeast Australia. Most of the continent displays $\rho > 0.4$, while there is also some regional clustering of $\rho \approx 0.3$. Generally $\rho > 0.2$ were found to be statistically significant ($p < 0.05$) correlations. A time series for the northeast, which is also a water–limited region, further corroborates the strong correlations there (Figure 1d). Vegetation dynamics reflecting water storage in arid and semi–arid regions is to be expected; however, the strong similarity between $\widehat{\text{EWT}}$ and $\widehat{\text{NDVI}}$ time series is striking.

[12] Linear trends in $\widehat{\text{EWT}}$ and EWT show an area of significantly declining water storage for the period 2002–2010 which spans the continent from the northwest to the southeast (Figures 2a and 2b). Note, those areas shaded gray in each of the panels of Figure 2 were the statistically insignificant trends. In northwest Australia the normalized trend is as low as -12% yr^{-1} and thus accounts for 96% of the observed range of variation in stored water over the eight years of observation. In absolute terms, GRACE-derived estimates of water losses of the order of 32 mm yr^{-1} occurred in an area adjacent to and including the Great Sandy, Tanami and Gibson deserts in northwest Australia (Figure 2b). Unfortunately there are few rain gauge measurements in this region to ground truth this result. In southeast Australia the fastest rates of water storage decline are of the order of 3% yr^{-1} or in absolute terms 36 mm yr^{-1}. This is comparable to previous estimates of water loss from the Murray Darling basin in southeast Australia of 29 mm yr^{-1} between 2002 and 2006, the majority of which was estimated to be from groundwater losses [*Leblanc et al.*, 2009].Total continental water loss, including areas of statistically insignificant trends located predominantly in the west, are of the order of 430 km^3 for this period while in areas with positive trends, located primarily in the north and north east, the gains total 159 km^3. The net rate of water loss from Australia is 34 km^3 yr^{-1}. In a global context, this is 52% of recent estimates of water loss from West Antarctica, or equivalently 5% of the contemporary rate of sea level rise [*Wu et al.*, 2010].

[13] Spatial patterns of significant trends in $\widehat{\text{NDVI}}$ correspond well with those for $\widehat{\text{EWT}}$ (Figure 2c). The finer resolution of the NDVI data elucidates a patchy distribution of areas with significant negative trends, which, together, encompass a coherent mosaic, primarily across the central and northwestern areas of the continent, with few areas of significant positive trends between. Both positive and negative vegetation trends are consistent with the pattern of rainfall trends (Figure 2d). Due to the dearth of rain gauges, the gridded rain data, produced from the rain gauge network, may be underestimating the full extent of rainfall declines. However, a recent comparison with satellite derived rainfall suggests a fairly good correlation between BoM and satellite gridded data sets in this region [*Fleming et al.*, 2011]. We can show, therefore, that the water storage drought largely correlates with an ecological stress, and both appear to have been driven by medium–term declines in rainfall. However, rates of rainfall declines cannot fully account for rates of water storage loss, particularly over northwest Australia. A linear regression between $\widehat{\text{NDVI}}$ trends (averaged at a 1° resolution) and $\widehat{\text{EWT}}$ trends found the slope, but not the intercept, to be significantly ($p < 0.01$) different from zero. The slope indicates that a unit rate of decline in water storage (yr^{-1}) occurs with a 0.29 ± 0.02 (yr^{-1}) rate of decline in $\widehat{\text{NDVI}}$. This estimate of vegetation-water relations across the continent however, should be interpreted with caution due to differences in the scale of measurements and correlated errors in EWT estimates [*Swenson and Wahr*, 2006].

[14] Fewer areas with significant negative NDVI trends were identified in southeast Australia, where water storage was in widespread decline. The intensive agricultural production there as well as the widespread use of irrigation may provide an explanation, while saturation of NDVI in forested areas may be a contributing factor. Alternatively, vegetation may have largely stabilized prior to 2002 as the drought there had been ongoing since approximately 1997

[1]Auxiliary materials are available in the HTML. doi:10.1029/2011GL050263.

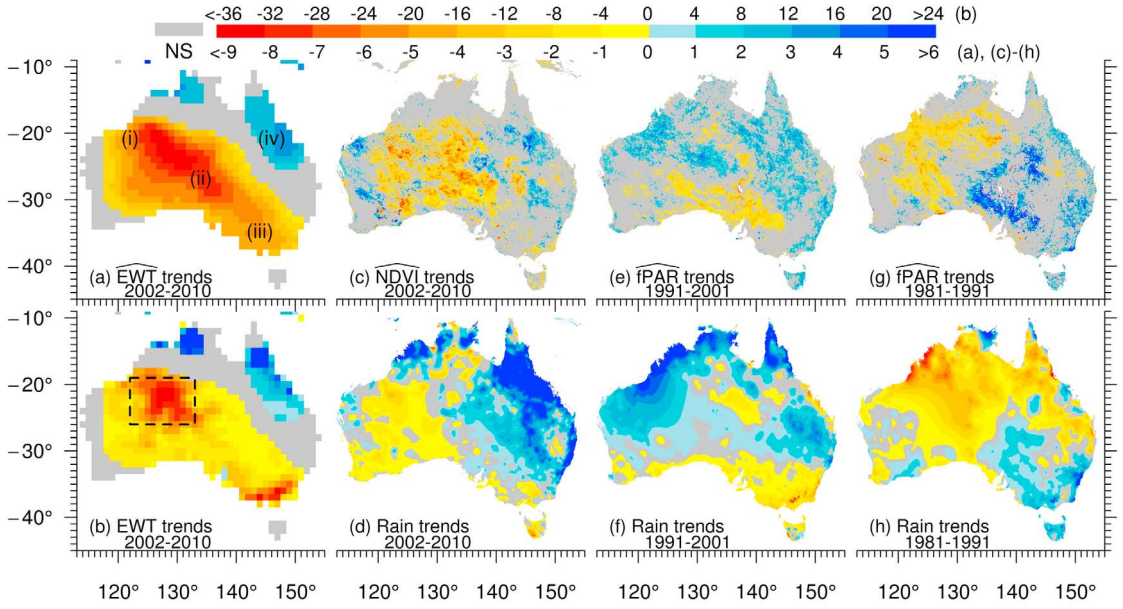

Figure 2. Magnitudes of significant trends in (a) normalized equivalent water thickness, $\widehat{EWT}$ (% yr^{-1}); (b) absolute equivalent water thickness, EWT (mm yr^{-1}); (c) normalized NDVI, $\widehat{NDVI}$ (% yr^{-1}); and (d) rainfall (mm yr^{-1}) for the period 2002–2010; as well as trends in (e, g) normalized fPAR, $\widehat{fPAR}$ (% yr^{-1}) and (f, h) rainfall (mm yr^{-1}) for two other tropical cyclone epochs. The roman numerals i–iv correspond to time series shown on Figures 1a–1d respectively while the rectangular region in Figure 2b relates to Figure 3. The gray shading and NS denotes areas with no statistically significant trend.

[*Ummenhofer et al.*, 2009]. In contrast, two areas in the north and northeast of the continent show increasing water storage of the order of 12 mm yr^{-1} and 9 mm yr^{-1} respectively or, in relative terms, 3% of the observed range per year. Positive NDVI trends are observed in the same areas, although significant increases in the northeast are more widespread. During the 1990's, extensive land clearing occurred in northeast Australia [*Donohue et al.*, 2009] which is also known to dramatically increase recharge rates [*Scanlon et al.*, 2006]. This, in addition to increasing rainfall, may be contributing to the positive gravity trend there.

[15] To investigate causes of the strong anomaly in northwest Australia (see rectangular region in Figure 2b) we analyzed smoothed time series of tropical cyclone numbers passing across the area, as well as smoothed time series of areal-mean rainfall and vegetation ($\widehat{fPAR}$) allowing a comparison back to 1981 (Figure 3). The 36 month moving averaged time series were found to be similar to smoothed time series estimated by generalized cross validation [*Wood*, 2004] although the latter allows for a more statistically defensible estimate of cross-correlations. Prior to the GRACE era, there was a period of relatively intensive cyclonic activity over northwest Australia, peaking in the year 2000, which has subsequently decreased (Figure 3). Peaks in cyclone numbers occurred in 1983, 1995 and 2000 coinciding with peaks in vegetation cover. While the rainfall increase was not as great in 1995, the large vegetation response might be explained by more effective recharge of water stores during cyclonic events than during non-cyclonic rainfall. Cyclones and rainfall decreased rapidly after 2000, however, vegetation reductions were initially subdued suggesting that the plants were utilizing stored water for transpiration. This is supported by the strong water losses measured since the GRACE mission started in 2002. The continent-wide pattern of trends during three phases of cyclone activity (1981–1991, 1991–2001 and 2002–2010) show that the trends across northwest Australia are mostly consistent with this pattern (Figures 2c–2h). Unlike the recent drought, rainfall and vegetation in the southeast had the opposite trends to those in the northwest during earlier phases of cyclone activity, suggesting that the recent continent–wide drought is the result of the coincident timing of two distinct climate drivers.

[16] Correlations between long term variation in fPAR, cyclones, rainfall, the Nino3.4 anomaly and DMI were assessed on smooth series derived from generalized cross validation. Vegetation (fPAR) was found to be strongly and positively correlated with rainfall (0.73) and cyclones (0.42), however contrary to the initial hypothesis, positive correlation was found with the DMI (0.57) and none with Nino3.4. Cyclone frequency was positively correlated with rainfall (0.60), as expected, and consistent with *Liu and Chan* [2010], we found a positive correlation between DMI and Nino3.4. While no significant correlation was found between Nino3.4 and fPAR for this area, simple models with multiple lags (in years) provided good correlations suggesting that the rate of change in Nino3.4 and DMI may be important for variation in fPAR. Variations in the occurrence of tropical cyclones appears to have a significant effect on vegetation in northwest Australia, however a link with conditions in southeast Australia remains unclear. Interactions between climate drivers, may be responsible for the continental scale drought. Recently, *Liu and Chan* [2010] demonstrated that more cyclones occur during La Niña than El Niño in northwest Australia, although within a La Niña, the state of the IOD does not significantly impact upon cyclone numbers. We also found a negative correlation between cyclone numbers and the Nino3.4 anomaly, as well

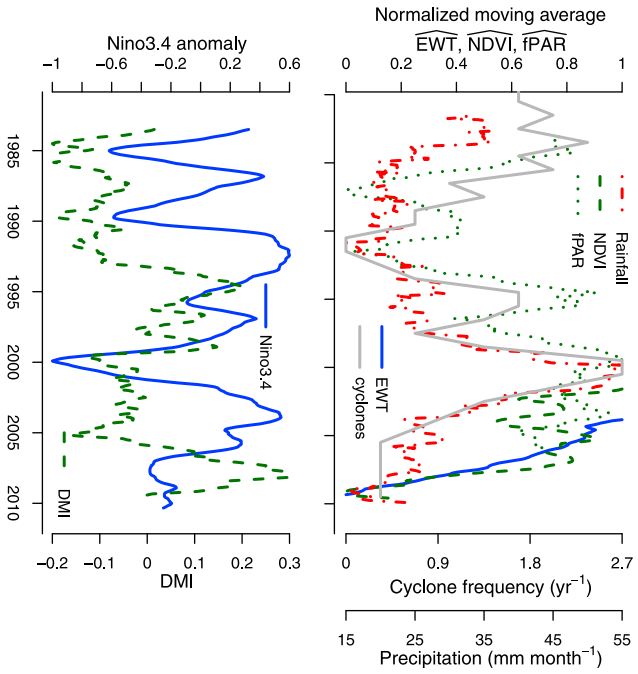

Figure 3. Three year moving averages of cyclone frequency, EWT, NDVI, fPAR, rainfall over the rectangular region shown in Figure 2b, as well as the Nino3.4 anomaly and DMI.

as a slight positive correlation with DMI, but both lacked statistical significance.

4. Conclusions

[17] The scientific focus on the drought in southeast Australia is not surprising, given the intensive agriculture and dense population there, in comparison to central and northwest Australia [*Leblanc et al.*, 2009]. However, it appears that a recent drought did in fact encompass most of the continent, which was not previously recognized. Decade-scale fluctuations in vegetation and rainfall in northwest Australia varies in conjunction with tropical cyclone frequency. The recent drought there is associated with a period of declining cyclone frequency. The Big Dry however has been attributed to inter-decadal variability in the Indian Ocean Dipole. The continent-wide drought therefore appears to be the result of coincident timing of separate but potentially correlated climate drivers. The reliance of ecosystems on tropical cyclones might also be seen in other arid zones fringing the tropics, such as southwest North America, as well as eastern Africa. Predicting the occurrence of tropical cyclones may therefore be essential to understanding the impact of climate change on these ecosystems.

[18] **Acknowledgments.** This research was supported under the Australian Research Council *Linkage Projects* (project LP0774881 in conjunction with Newcrest Mining Ltd. and Minerals and Energy Research Institute of Western Australia - project M381) and *Discovery Projects* (project DP0877381) funding schemes. GRACE land data were processed by Sean Swenson, supported by the NASA MEASURES program, and are available at http://grace.jpl.nasa.gov. K.F.'s contribution makes this a TIGeR (The Institute of Geoscience Research) publication (no. 399).

[19] The Editor wishes to thank two anonymous reviewers for their assistance evaluating this manuscript.

References

Abram, N. J., M. K. Gagan, J. E. Cole, W. S. Hantoro, and M. Mudelsee (2008), Recent intensification of tropical climate variability in the Indian Ocean, *Nat. Geosci.*, *1*, 849–853, doi:10.1038/ngeo357.

Ashok, K., Z. Guan, and T. Yamagata (2003), Influence of the Indian Ocean dipole on the Australian winter rainfall, *Geophys. Res. Lett.*, *30*(15), 1821, doi:10.1029/2003GL017926.

Cai, W., A. Sullivan, and T. Cowan (2009), Climate change contributes to more frequent consecutive positive Indian Ocean Dipole events, *Geophys. Res. Lett.*, *36*, L23704, doi:10.1029/2009GL040163.

Cullen, L. E., and P. F. Grierson (2007), A stable oxygen, but not carbon, isotope chronology of Callitris columellaris reflects recent climate change in north-western Australia, *Clim. Change*, *85*, 213–229, doi:10.1007/s10584-006-9206-3.

Donohue, R. J., M. L. Roderick, and T. R. McVicar (2008), Deriving consistent long-term vegetation information from AVHRR reflectance data using a cover-triangle-based framework, *Remote Sens. Environ.*, *112*, 2938–2949, doi:10.1016/j.rse.2008.02.008.

Donohue, R. J., T. R. McVicar, and M. Roderick (2009), Climate-related trends in Australian vegetation cover as inferred from satellite observations, 1981–2006, *Global Change Biol.*, *15*, 1025–1039, doi:10.1111/j.1365-2486.2008.01746.x.

Fleming, K., J. L. Awange, M. Kunh, and W. E. Featherstone (2011), Evaluating the TRMM 3B43 monthly precipitation product using gridded raingauge data over Australia, *Aust. Meteorol. Oceanograph. J.*, *61*, 171–184.

Goebbert, K. H., and L. M. Leslie (2010), Interannual variability of northwest Australian tropical cyclones, *J. Clim.*, *23*, 4538–4555, doi:10.1175/2010JCLI3362.1.

Hassim, M. E. E., and K. J. E. Walsh (2008), Tropical cyclone trends in the Australian region, *Geochem. Geophys. Geosyst.*, *9*, Q07V07, doi:10.1029/2007GC001804.

Huete, A., K. Didan, T. Miura, E. P. Rodriguez, X. Gao, and L. G. Ferreira (2002), Overview of the radiometric and biophysical performance of the MODIS vegetation indices, *Remote Sens. Environ.*, *83*, 195–213, doi:10.1016/S0034-4257(02)00096-2.

Ihara, C., Y. Kushnir, and M. A. Cane (2008), Warming trend of the Indian Ocean SST and Indian Ocean Dipole from 1880 to 2004, *Bull. Am. Meteorol. Soc.*, *21*, 2035–2046, doi:10.1175/2007JCLI1945.1.

King, E. A. (2003), The Australian AVHRR data set at CSIRO/EOC: Origins, processes, holdings and prospects, *Rep. 2003/04*, CSIRO Earth Obs. Cent., Canberra, ACT, Australia.

Leblanc, M. J., P. Tregoning, G. Ramillien, S. O. Tweed, and A. Fakes (2009), Basin-scale, integrated observations of the early 21st century multiyear drought in southeast Australia, *Water Resour. Res.*, *45*, W04408, doi:10.1029/2008WR007333.

Liu, K. S., and J. C. L. Chan (2010), Interannual variation of Southern Hemisphere tropical cyclone activity and seasonal forecast of tropical cyclone number in the Australian region, *Int. J. Climatol.*, doi:10.1002/joc.2259, in press.

Nott, J. (2010), A 6000 year tropical cyclone record from Western Australia, *Quat. Sci. Rev.*, *30*(5–6), 713–722, doi:10.1016/j.quascirev.2010.12.004.

Rieser, D., M. Kuhn, R. Pail, I. M. Anjasmara, and J. Awange (2010), Relation between GRACE-derived surface mass variations and precipitation over Australia, *Aust. J. Earth. Sci.*, *57*, 887–900, doi:10.1080/08120099.2010.512645.

Scanlon, B. R., K. E. Keese, A. L. Flint, L. E. Flint, C. B. Gaye, W. M. Edmunds, and I. Simmers (2006), Global synthesis of groundwater recharge in semiarid and arid regions, *Hydrol. Processes*, *20*, 3335–3370, doi:10.1002/hyp.6335.

Smith, I., and B. Timbal (2012), Links between tropical indices and southern Australia rainfall, *Int. J. Climatol.*, *32*, 33–40, doi:10.1002/joc.2251.

Swenson, S. C., and J. Wahr (2006), Post-processing removal of correlated errors in GRACE data, *Geophys. Res. Lett.*, *33*, L08402, doi:10.1029/2005GL025285.

Taschetto, A. S., and M. H. England (2009), An analysis of late twentieth century trends in Australia rainfall, *Int. J. Climatol.*, *29*, 791–807, doi:10.1002/joc.1736.

Ummenhofer, C. C., M. H. England, P. C. McIntosh, G. A. Meyers, M. J. Pook, J. S. Risbey, A. S. Gupta, and A. S. Taschetto (2009), What causes southeast Australia's worst droughts?, *Geophys. Res. Lett.*, *36*, L04706, doi:10.1029/2008GL036801.

Wahr, J., S. Swenson, V. Zlotnicki, and I. Velicogna (2004), Time–variable gravity from GRACE: First results, *Geophys. Res. Lett.*, *31*, L11501, doi:10.1029/2004GL019779.

Wood, S. N. (2004), Stable and efficient multiple smoothing parameter estimation for generalized additive models, *J. Am. Stat. Assoc.*, *99*, 673–686.

Wu, X., M. B. Heflin, H. Schotman, B. L. A. Vermeersen, D. Dong, R. S. Gross, E. R. Ivins, A. W. Moore, and S. E. Owen (2010),

Simultaneous estimation of global present-day water transport and glacial isostatic adjustment, *Nat. Geosci.*, *3*(9), 642–646, doi:10.1038/ngeo938.
Xu, Z. X., K. Takeuchi, H. Ishidaira, and J. Y. Li (2005), Long-term trend analysis for precipitation in Asian Pacific FRIEND river basins, *Hydrol. Processes*, *19*, 3517–3532, doi:10.1002/hyp.5846.

K. Fleming, Earthquake Risk and Early Warning, Helmholtz Centre Potsdam, GFZ German Research Centre for Geosciences, D-14467 Potsdam, Germany.
C. Hinz, Hydrology and Water Resources Management, Brandenburg University of Technology, Konrad-Wachsmann-Allee 6, D-03046 Cottbus, Germany.
G. S. McGrath, School of Earth and Environment, University of Western Australia, M087, 35 Stirling Hwy., Crawley, WA 6009, Australia. (gavan.mcgrath@uwa.edu.au)
R. Sadler, School of Agricultural and Resource Economics, University of Western Australia, M089, 35 Stirling Hwy., Crawley, WA 6009, Australia.
P. Tregoning, Research School of Earth Sciences, Australian National University, Canberra, ACT 0200, Australia.
E. J. Veneklaas, School of Plant Biology, University of Western Australia, M084, 35 Stirling Hwy., Crawley, WA 6009, Australia.